Directed polymer in a random medium of dimension 1+3: Multifractal properties at the localization-delocalization transition

Cécile Monthus and Thomas Garel
Service de Physique Théorique, CEA/DSM/SPhT, Unité de recherche associée au CNRS, 91191 Gif-sur-Yvette cedex, France
(Received 30 January 2007; published 30 May 2007)

We consider the model of the directed polymer in a random medium of dimension 1+3, and investigate its multifractal properties at the localization-delocalization transition. In close analogy with models of the quantum Anderson localization transition, where the multifractality of critical wavefunctions is well established, we analyze the statistics of the position weights $w_L(\vec{r})$ of the endpoint of the polymer of length L via the moments $Y_q(L)=\Sigma_{\vec{r}}[w_L(\vec{r})]^q$. We measure the generalized exponents $\tau(q)$ and $\tilde{\tau}(q)$ governing the decay of the typical values $Y_q^{\rm typ}(L)=e^{\overline{\ln Y_q(L)}}\sim L^{-\tau(q)}$ and disorder-averaged values $\overline{Y_q(L)}\sim L^{-\tilde{\tau}(q)}$, respectively. To understand the difference between these exponents, $\tau(q)\neq\tilde{\tau}(q)$ above some threshold $q>q_c\sim 2$, we compute the probability distributions of $y=Y_q(L)/Y_q^{\rm typ}(L)$ over the samples: We find that these distributions becomes scale invariant with a power-law tail $1/y^{1+x_q}$. These results thus correspond to the Evers-Mirlin scenario [Phys. Rev. Lett. **84**, 3690 (2000)] for the statistics of inverse participation ratios at the Anderson localization transitions. Finally, the finite-size scaling analysis in the critical region yields the correlation length exponent $\nu\sim 2$.

DOI: 10.1103/PhysRevE.75.051122 PACS number(s): 02.50.−r, 05.40.−a, 05.45.Df

I. INTRODUCTION

The notion of multifractals is now important in various areas of physics (see, for instance [1–7] and references therein). For classical systems with frozen disorder of interest here, the idea that multifractality is present at criticality has been mostly investigated for correlation functions in two-dimensional diluted ferromagnets [8–12], spin-glasses and random field spin systems [13–15]. For disordered quantum spin-chains, the statistics of critical correlation functions is described by "multiscaling," which is even stronger than multifractality [16]. For quantum localization models, the multifractality of the critical wavefunction shows up through the statistics of inverse participation ratios (I.P.R.s) [17,18]. Many results are now available for the Anderson localization transition in $d=3$ [19–22], the integer quantum Hall transition [23,24] Dirac fermions in a random magnetic field [25], and power-law random banded matrices [26]. Connections have been also established with the scaling properties of the correlation functions [27] and with the time evolution of wave packets [28]. More recently, it was realized that typical and disorder-averaged I.P.R.s can actually lead to two different multifractal spectra as a consequence of the broadness of their probability distributions [21,26,29].

In this paper, we consider the localization-delocalization transition of the directed polymer in a random medium of dimension 1+3 (see the review [30] and references therein), to investigate whether some multifractality in present at criticality, in analogy with the quantum localization models quoted above. Note that at the level of one-loop renormalization-group calculation in dimension $d=2+\epsilon$, multifractality is already present both for the directed polymer [31] and for Anderson localization [17].

The paper is organized as follows. In Sec. II, we introduce the directed polymer model and the observables displaying multifractal behavior at criticality. We then describe our numerical results concerning the generalized dimensions $D(q)$ and $\tilde{D}(q)$ that govern typical and averaged values (Sec. III), the singularity spectrum (Sec. IV), and the probability distributions over the samples (Sec. V). Finally, we present in Sec. VI the finite-size scaling analysis in the critical region. Section VII contains our conclusions.

II. MODELS AND OBSERVABLES

A. Model definition

The random bond directed polymer model [30] is defined by the following recursion relation for the partition function on the cubic lattice in $d=3$

$$Z_{t+1}(\vec{r})=\sum_{j=1}^{2d} e^{-\beta\epsilon_t(\vec{r}+\vec{e}_j,\vec{r})}Z_t(\vec{r}+\vec{e}_j). \tag{1}$$

The bond energies $\epsilon_t(\vec{r}+\vec{e}_j,\vec{r})$ are random independent variables drawn from the Gaussian distribution

$$\rho(\epsilon)=\frac{1}{\sqrt{2\pi}}e^{-\epsilon^2/2}. \tag{2}$$

In this paper, we consider the following boundary conditions. The first monomer is fixed at $\vec{r}=\vec{0}$, i.e., the initial condition of the recurrence of Eq. (1) reads

$$Z_{t=0}(\vec{r})=\delta_{\vec{r},\vec{0}}. \tag{3}$$

The last monomer is free, i.e., the full partition function of the polymer of length L is then obtained by summing over all possible positions $\vec{r}$ at $t=L$

$$Z_L^{\rm tot}=\sum_{\vec{r}} Z_L(\vec{r}). \tag{4}$$

The phase diagram of this directed polymer model as a function of space dimension d is the following [30]. In dimension $d\leqslant 2$, there is no free phase, i.e., any initial disorder drives the polymer into a strong disorder phase, where the order parameter is an "overlap" [32–36]. In dimension, d

>2, there exists a phase transition between the low temperature disorder dominated phase and a free phase at high temperature [37–39]. This phase transition has been studied exactly on a Cayley tree [32]. In finite dimensions, bounds on the critical temperature T_c have been derived [38,40,41]: $T_0(d) \leqslant T_c \leqslant T_2(d)$. The upper bound $T_2(d)$ corresponds to the temperature above which the ratio $\overline{Z_L^2}/(\overline{Z_L})^2$ remains finite as $L \to \infty$. The lower bound T_0 corresponds to the temperature below which the annealed entropy becomes negative. On the Cayley tree, the critical temperature T_c coincides with T_0 [32]. In finite dimensions however, we have argued in [42] that T_c coincides with T_2, and our recent numerical simulations [43] are in agreement with the numerical value given in [40] for $T_2(d=3)$:

$$T_c = T_2(d=3) = 0.790. \tag{5}$$

The numerical results given below have been obtained using polymers of various lengths L, with corresponding numbers $n_s(L)$ of disordered samples with

$$L = 6,12,18,24,36,48,60,72,84,96, \tag{6}$$

$$n_s(L) = 10^8, 10^7, 2.10^6, 8.10^5, 2.10^5, 5.10^4, 3.10^4, 2.10^4, 4.10^4, 2.10^4. \tag{7}$$

In the following, $\bar{A}$ denotes the average of A over the disorder samples. We also define $(\Delta A)^2 = \overline{A^2} - \bar{A}^2$.

B. Notion of multifractal statistics at criticality

In this paper, we will focus on the statistical properties of the weights

$$w_L(\vec{r}) = \frac{Z_L(\vec{r})}{Z_L^{\rm tot}} \tag{8}$$

normalized to [Eq. (4)]

$$\sum_{\vec{r}} w_L(\vec{r}) = 1 \tag{9}$$

and study whether they present some multifractal properties at criticality. We thus consider the following moments of arbitrary order q

$$Y_q(L) = \sum_{\vec{r}} w_L^q(\vec{r}) \tag{10}$$

that are the dynamical analogs of the inverse participation ratios (I.P.R.s) in quantum localization models [26]

$$P_q(L) = \int_{L^d} d^d\vec{r} |\psi(\vec{r})|^{2q}. \tag{11}$$

As a consequence of the normalization of Eq. (9), one has the identity $Y_{q=1}(L)=1$. The localization/delocalization transition can be characterized by the asymptotic behavior in the limit $L \to \infty$ of the $Y_q(L)$ for $q>1$. In the localized phase $T<T_c$ these moments $Y_q(L)$ converge to finite values

$$Y_q(L=\infty) > 0 \text{ for } T < T_c. \tag{12}$$

In the delocalized phase, the spreading of the polymer involves the Brownian exponent $\zeta = 1/2$, and, space being of dimension $d=3$, the decay of the moments follows the scaling

$$Y_q(L) \simeq L^{-(q-1)d\zeta} = L^{-(q-1)(3/2)} \text{ for } T > T_c. \tag{13}$$

Exactly at criticality, the typical decay of the $Y_q(L)$ defines a series of generalized exponents $\tau(q) = (q-1)D(q)$

$$Y_q^{\rm typ}(L) \equiv e^{\overline{\ln Y_q(L)}}|_{T=T_c} \simeq L^{-\tau(q)} = L^{-(q-1)D(q)}. \tag{14}$$

The notion of multifractality corresponds to the case where $D(q)$ depends on q, whereas monofractality corresponds to $D(q)=$cst as in Eq. (13). The exponents $D(q)$ represent generalized dimensions [1]: $D(0)$ represent the dimension of the support of the measure, here it is simply given by the space dimension $D(0)=d=3$; $D(1)$ is usually called the information dimension [1], since it describes the behavior of the "information" entropy

$$s_L \equiv -\sum_{\vec{r}} w_L(\vec{r}) \ln w_L(\vec{r}) = -\partial_q Y_q(L)|_{q=1} \simeq D(1) \ln L. \tag{15}$$

Finally $D(2)$ is called the correlation dimension [1] and describes the decay of

$$Y_2^{\rm typ}(L) \equiv e^{\overline{\ln Y_2(L)}}|_{T=T_c} \simeq L^{-D(2)}. \tag{16}$$

In the multifractal formalism, the singularity spectrum $f(\alpha)$ is given by the Legendre transform of $\tau(q)$ [1] via the standard formulas

$$q = f'(\alpha), \tag{17}$$

$$\tau(q) = \alpha q - f(\alpha). \tag{18}$$

The physical meaning of $f(\alpha)$ is that the number $\mathcal{N}_L(\alpha)$ of points $\vec{r}$ where the weight $w_L(\vec{r})$ scales as $L^{-\alpha}$ typically behaves as

$$\mathcal{N}_L(\alpha) \propto L^{f(\alpha)}. \tag{19}$$

So the Legendre transform of Eq. (18) corresponds to the saddle-point calculus in α of the following expression:

$$Y_q^{\rm typ}(L) \sim \int d\alpha L^{f(\alpha)} L^{-q\alpha}. \tag{20}$$

The general properties of the singularity spectrum $f(\alpha)$ are as follows [1]: It is positive $f(\alpha) \geqslant 0$ on an interval $[\alpha_{\min}, \alpha_{\max}]$ where $\alpha_{\min} = D(q=+\infty)$ is the minimal singularity exponent and $\alpha_{\max} = D(q=-\infty)$ is the maximal singularity exponent. It is concave $f''(\alpha) < 0$. It has a single maximum at some value α_0 where $f(\alpha_0) = D(q=0)$ [so here $f(\alpha_0)=3$], and contains the point $\alpha_1 = f(\alpha_1) = D(1)$.

Following [1], many authors consider that the singularity spectrum has a meaning only for $f(\alpha) \geqslant 0$ [19,20,23–25]. However, when multifractality arises in random systems, disorder-averaged values may involve other generalized ex-

ponents [44–47] than the typical values [see Eq. (14)]. In quantum localization transitions, these exponents were denoted by $\tilde{\tau}(q)=(q-1)\tilde{D}(q)$ in [26,29]

$$\overline{Y_q(L)|_{T=T_c}} \simeq L^{-\tilde{\tau}(q)} = L^{-(q-1)\tilde{D}(q)}. \tag{21}$$

For these disorder averaged values, the corresponding singularity spectrum $\tilde{f}(\alpha)$ may become negative $\tilde{f}(\alpha)<0$ [26,29,44–47] to describe rare events [cf. Eq. (19)]. The difference between the two generalized exponents sets $D(q)$ and $\tilde{D}(q)$ associated to typical and averaged values has for origin the broad distributions at criticality [21,26] as we now describe.

C. Probability distributions of the $Y_q(L)$

The scenario proposed in [21,26] in the context of quantum localization models is as follows: The probability distribution of the logarithm of the inverse participation ratios of Eq. (11) becomes scale invariant around its typical value [21,26], i.e.,

$$\ln P_q(L) = \overline{\ln P_q(L)} + u, \tag{22}$$

where u remains a random variable of order $O(1)$ in the limit $L\to\infty$. According to [26] the probability distribution $G_L(u)$ generically develops an exponential tail

$$G_\infty(u) \underset{u\to\infty}{\simeq} e^{-x_q u}. \tag{23}$$

As a consequence, the ratio $y=P_q(L)/P_q^{\rm typ}(L)=e^u$ with respect to the typical value $P_q^{\rm typ}(L)=e^{\overline{\ln P_q(L)}}$ presents the power-law decay

$$\Pi\left(y \equiv \frac{P_q(L)}{P_q^{\rm typ}(L)}\right) \propto_{y\to\infty} \frac{1}{y^{1+x_q}}. \tag{24}$$

The conclusions of [21,26] are then as follows: For q small enough $q<q_c$, the exponent satisfies $x_q>1$, and the corresponding generalized dimensions coincide $\tilde{D}(q)=D(q)$. However, for larger values $q>q_c$, the exponent $x(q)$ may become smaller $x(q)<1$, and then the corresponding generalized dimensions differ $\tilde{D}(q)\neq D(q)$: The decay of the averaged value $\overline{P_q(L)}$ is then determined by the finite-size cutoff of the power-law tail. In this case, the averaged values are not representative but are governed by rare events.

In this paper, we show that this scenario for the I.P.R.'s statistics at Anderson transitions describes well our data for the directed polymer at criticality.

III. RESULTS FOR THE GENERALIZED EXPONENTS $D(q)$ and $\tilde{D}(q)$

We show on Fig. 1(a) our results for the generalized exponents $D(q)$ and $\tilde{D}(q)$ governing the decay of typical and disorder averaged values [Eqs. (14) and (21)]. In agreement with the scenario proposed in [21,26] for Anderson transitions, we find that there exists a threshold q_c, of order $q_c\sim 2$ here, such that

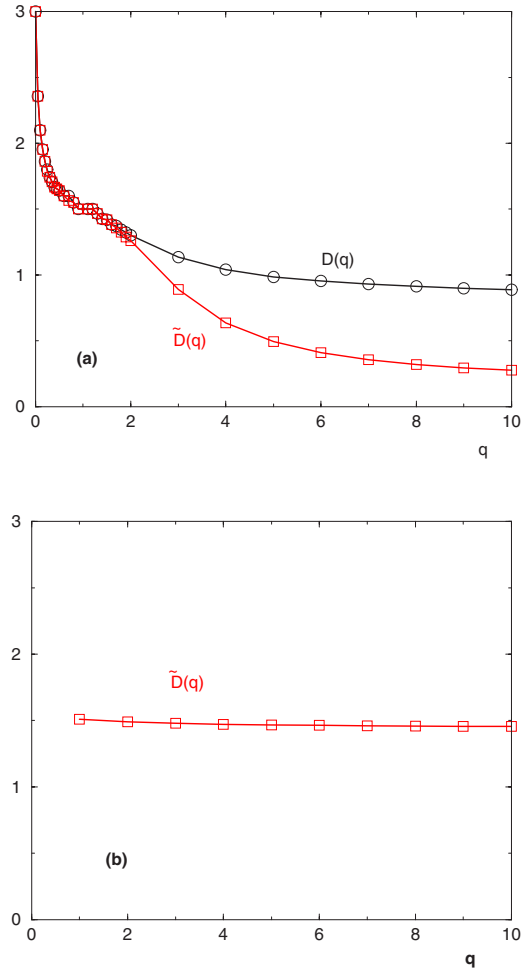

FIG. 1. (Color online) (a) Multifractality at criticality ($T=0.79$): Generalized dimensions $D(q)$ (○) and $\tilde{D}(q)$ (□) associated to typical and disorder averaged values [Eqs. (14) and (21)]. (b) Monofractality in the high-temperature phase ($T=2$): $D(q)=\tilde{D}(q)=\frac{3}{2}$ [see Eq. (13)].

$$D(q) = \tilde{D}(q) \text{ for } q < q_c, \tag{25}$$

$$D(q) > \tilde{D}(q) \text{ for } q > q_c. \tag{26}$$

In particular, for $q=1$, the information dimension of Eq. (15) is

$$D(1) = \tilde{D}(1) \sim 1.5 \tag{27}$$

and corresponds to the monofractal dimension $D_{T>T_c}(q)=3/2$ of the delocalized phase [see Eq. (13)], as numerically checked on Fig. 1(b).

For $q=2$, the correlation dimension $D(2)$ defined in Eq. (16) is found to be of order

$$D(2) \sim \tilde{D}(2) \sim 1.3. \tag{28}$$

For $q\geqslant 3$, the values for $D(q)$ and $\tilde{D}(q)$ are clearly different, in particular for $q=3$

$$D(3) \sim 1.1, \tag{29}$$

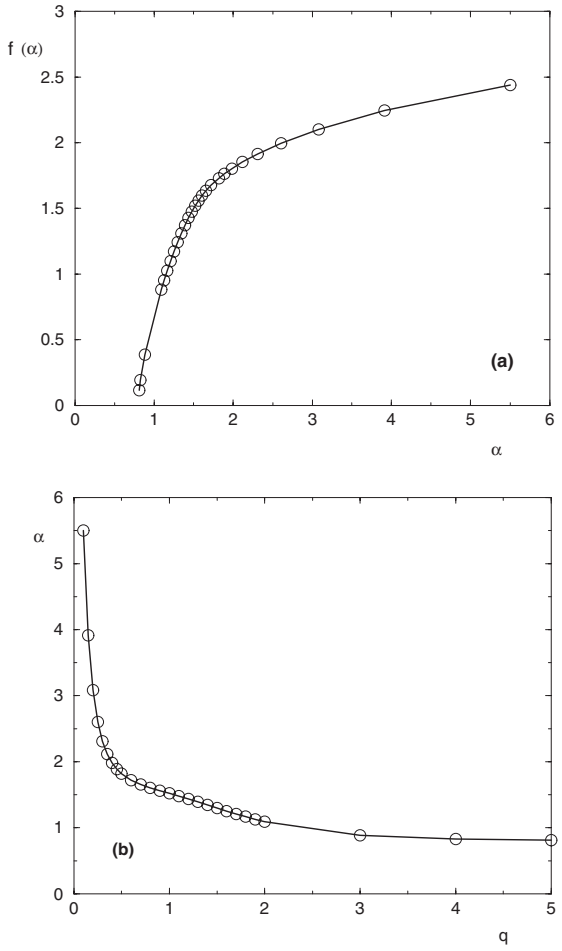

FIG. 2. (a) Singularity spectrum $f(\alpha)$: Starting at some $\alpha_{\min}=D(q=+\infty)\sim 0.77$ where $f(\alpha_{\min})=0$, it is tangent to the diagonal $\alpha=f(\alpha)$ at $\alpha_1=D(1)\sim 1.5$ and asymptotically goes to $f(+\infty)=D(0)=3$. (b) Corresponding curve $\alpha(q)$: Diverging at $q\to 0$, it goes through the point $\alpha(q=1)=D(1)\sim 1.5$ and tends to $\alpha_{\min}=D(q=+\infty)$ as $q\to\infty$.

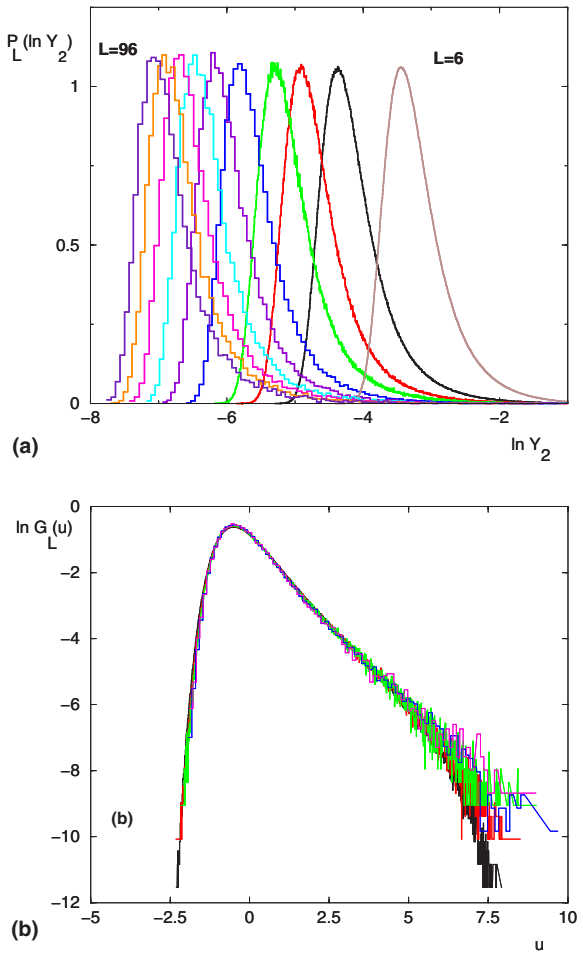

FIG. 3. (Color online) Histogram of $\ln Y_2(L)$ at criticality ($T_c=0.79$). (a) Probability distribution $P_L(\ln Y_2)$ for $L=6$, 12, 18, 24, 36, 48, 60, 72, 84, and 96. (b) Rescaled distributions $\ln G_L[u=\ln Y_2(L)-\overline{\ln Y_2(L)}]$: The exponential tail of Eq. (41) is clearly visible, the corresponding slope being $x_2\sim 1$.

$$\tilde{D}(3)\sim 0.9 \tag{30}$$

and for $q=10$

$$D(10)\sim 0.9, \tag{31}$$

$$\tilde{D}(10)\sim 0.3. \tag{32}$$

The limit $q\to\infty$ will be discussed more precisely below [see Eq. (39)].

Finally, for $q<0$, we find that $Y_q^{\mathrm{typ}}(L)$ and $\overline{Y_q(L)}$ diverge more rapidly than the power laws of Eqs. (14) and (21), i.e.,

$$D(q<0)=+\infty. \tag{33}$$

This can be understood in the delocalized phase $T>T_c$ where it is also true, since for the free Gaussian probability $w_{T=\infty}(\vec{r})\sim e^{-(\vec{r})^2/L}/L^{3/2}$ at $T=\infty$ leads to exponential divergence of Y_q in the negative region $q<0$. This finding for our "dynamical" model is thus very natural, but is a major difference with the Anderson localization cases where the generalized exponents $D(q)$ are finite for $q<0$.

IV. RESULTS FOR THE SINGULARITY SPECTRUM $f(\alpha)$

To measure the singularity spectrum $f(\alpha)$, we have followed the method of the q measures proposed in [48]. As explained above, in the negative region $q<0$, our model does not lead to power law [see Eq. (33)]. As a consequence, the maximum $[\alpha_0, f(\alpha_0)]$ of the curve $f(\alpha)$ which is at finite distance in Anderson localization models, is rejected towards infinity in our case

$$\alpha_0=+\infty, \tag{34}$$

$$f(\alpha_0)=D(q=0)=3. \tag{35}$$

Our result for the curve $f(\alpha)$ are shown on Fig. 2(a): It begins at some $\alpha_{\min}=D(q=+\infty)$ where $f(\alpha_{\min})=0$, it is tangent to the diagonal at $\alpha_1=D(1)\sim 1.5$, and asymptotically goes to $f(+\infty)=D(0)=3$.

The q values used in our computations and the corresponding $\alpha(q)$ [see Eq. (20)] are shown on Fig. 2(b).

To measure better the minimal exponent $\alpha_{\min}=D(q=+\infty)$ where $f(\alpha)$ vanishes $f(\alpha_{\min}=0)=0$, we have

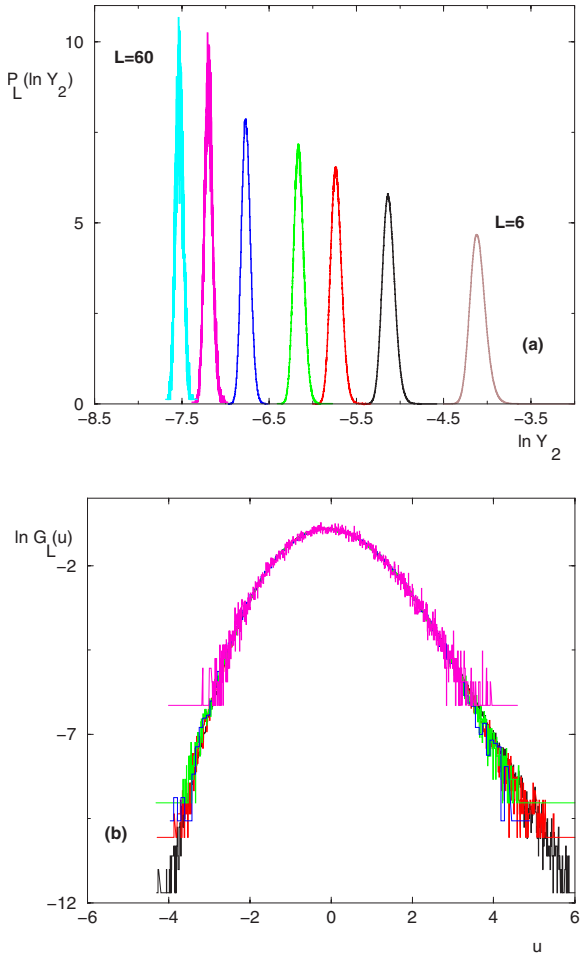

FIG. 4. (Color online) Histogram of $\ln Y_2(L)$ in the high-temperature phase ($T=2$). (a) Probability distribution of $P_L(\ln Y_2)$ for $L=6$, 12, 18, 24, 36, 48, and 60. (b) The distributions $G_L(u)$ of the rescaled variable $u=[\ln Y_2(L)-\overline{\ln Y_2(L)}]/[\Delta \ln Y_2(L)]$ become Gaussian.

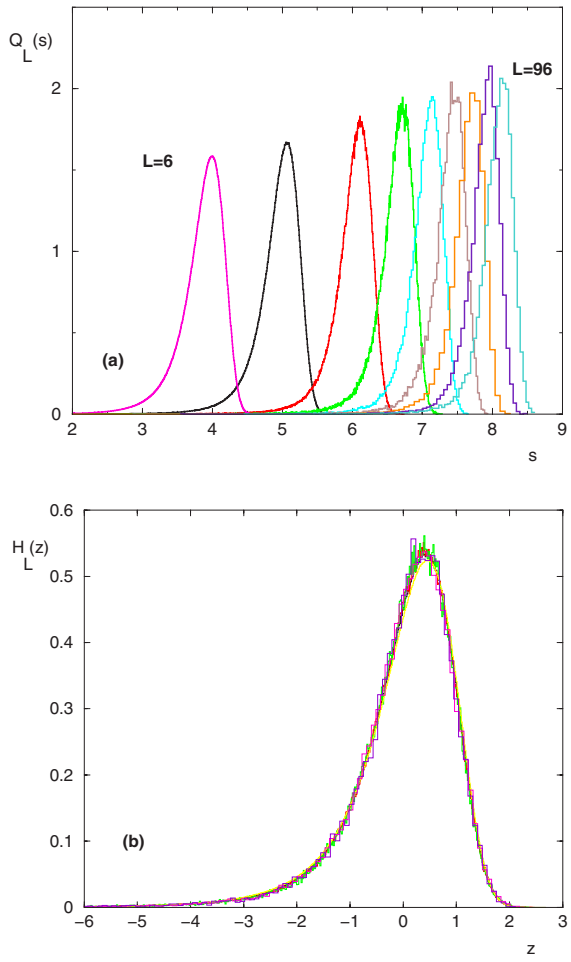

FIG. 5. (Color online) Histogram of the entropy $s_L=-\Sigma_{\vec{r}} w_L(\vec{r})\ln w_L(\vec{r})$ at criticality ($T=0.79$). (a) Probability distribution $Q_L(s)$ for $L=6$, 12, 24, 36, 48, 60, 72, 84, and 96. (b)The distributions $H_L(z)$ of the rescaled variable $z=(s_l-\overline{s_L})/\Delta s_L$ are clearly asymmetric.

studied the statistics of the maximal weight in each sample [Eq. (8)]

$$w_L^{\max} = \max_{\vec{r}}[w_L(\vec{r})]. \tag{36}$$

The disorder-averaged value of its logarithm gives

$$\overline{\ln w_L^{\max}} \sim -0.77 \ln L. \tag{37}$$

The first moment involves a similar value

$$\overline{w_L} \sim L^{-0.75} \tag{38}$$

so our conclusion is that the minimal exponent in a typical sample is around

$$\alpha_{\min} = D(q=+\infty) \sim 0.77. \tag{39}$$

V. RESULTS FOR PROBABILITY DISTRIBUTIONS

A. Probability distributions of the $Y_q(L)$

To understand the difference between the generalized exponents associated to typical and averaged values [Eq. (26)], we now consider the probability distributions of $Y_q(L)$ over the samples. Our results for the histograms of $\ln Y_2(L)$ for various L at criticality are shown on Fig. 3(a). Remarkably, as L grows, this distribution simply shifts along the x axis with a fixed shape, as also found in [21,26] for I.P.R.s at Anderson transitions. As in Eq. (22), we may therefore write

$$\ln Y_q(L) = \overline{\ln Y_q(L)} + u, \tag{40}$$

where u is a random variable of order $O(1)$ in the limit $L \to \infty$. The probability distribution $G_2(u)$ of $u=\ln Y_2(L) - \overline{\ln Y_2(L)}$ is shown on Fig. 3(b) for various L. It clearly develops an exponential tail as $u \to \infty$

$$G_{L\to\infty}(u) \underset{u\to\infty}{\simeq} e^{-x_q u}. \tag{41}$$

As stressed in [21,26], the ratio $y=Y_q(L)/Y_q^{\text{typ}}(L)=e^u$ then presents the power-law decay

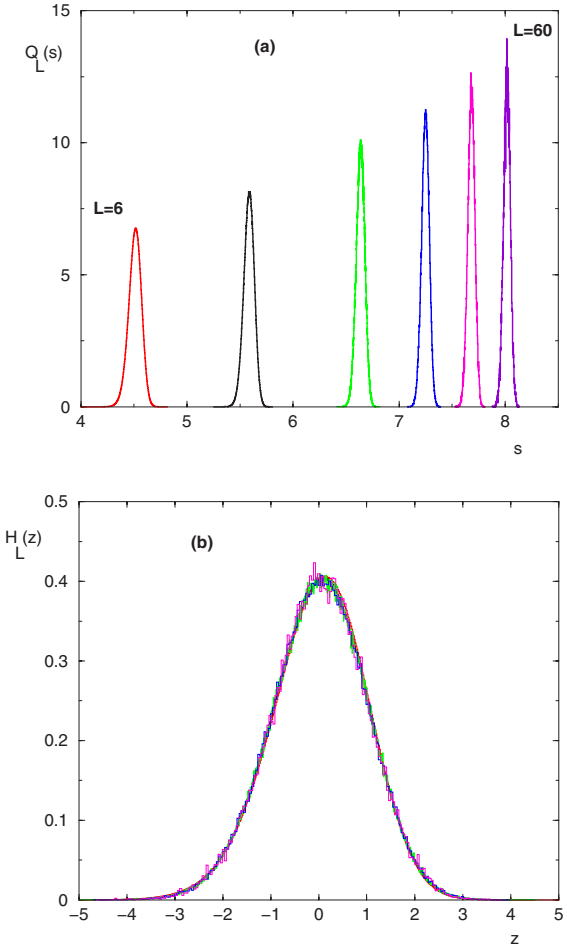

FIG. 6. (Color online) Histogram of the entropy $s_L=-\Sigma_{\vec{r}} w_L(\vec{r})\ln w_L(\vec{r})$ in the high temperature phase ($T=2$). (a) Probability distribution $Q_L(s)$ for $L=6$, 12, 24, 36, 48, and 60. (b) The distributions $H_L(z)$ of the rescaled variable $z=(s_l-\overline{s_L})/\Delta s_L$ become Gaussian.

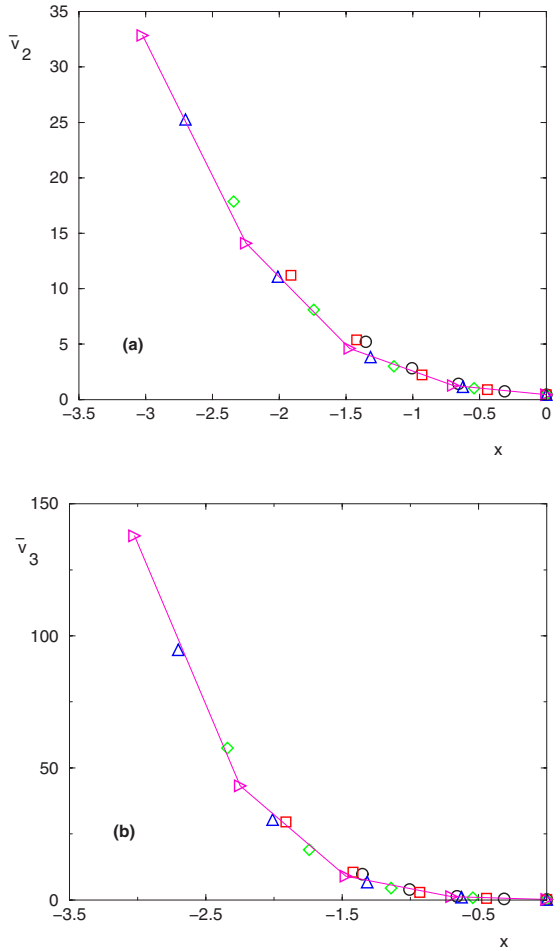

FIG. 7. (Color online) Finite-size scaling ($T<T_c$) of $\overline{v_q}=L^{\tilde{\tau}(q)}\overline{Y_q}$ as a function of $x=(T-T_c)L^{1/\nu}$, see Eq. (43), with the value $\nu=2$ and for the sizes $L=12(\bigcirc)$, $24(\square)$, $36(\diamond)$, $48(\triangle)$, and $60(\triangleright)$. (a) $q=2$; (b) $q=3$.

$$\Pi\left(y \equiv \frac{Y_q(L)}{Y_q^{\mathrm{typ}}(L)}\right) \underset{y\to\infty}{\propto} \frac{1}{y^{1+x_q}}. \tag{42}$$

Whenever $x_q<1$, the corresponding generalized dimensions differ $\tilde{D}(q)\neq D(q)$ [Eq. (26)]: The decay of the averaged value $\overline{Y_q(L)}$ is then determined by the finite-size cutoff of the power-law tail. Our results for the histograms of $Y_q(L)$ for $q=3,4,\ldots$ are similar to the results shown for $q=2$ on Fig. 3.

For comparison, we show on Fig. 4(a) the histogram of $\ln Y_2(L)$ in the delocalized phase at $T=2$: As L grows, the width shrinks around the averaged value $\overline{\ln Y_2(L)}\sim -(3/2)\ln L$. The corresponding rescaled distribution shown on Fig. 4(b) tends towards the Gaussian distribution.

B. Probability distributions of the last-monomer entropy $s_L=-\Sigma_{\vec{r}} w_L(\vec{r})\ln w_L(\vec{r})$

Since the last-monomer entropy s_L is closely related to the $Y_q(L)$ [Eq. (15)], we have also computed its histogram over the samples both at criticality (Fig. 5) and in the delocalized phase at $T=2>T_c$ [Fig. 6]. Again, the rescaled distribution is Gaussian for $T>T_c$ [Fig. 6(b)], and strongly asymmetric at criticality [Fig. 5(b)].

VI. FINITE-SIZE SCALING IN THE CRITICAL REGION

For Anderson transitions, finite-size scaling involves the multifractal spectrum at criticality but a single correlation length exponent ν (see the reviews [23,24]). In this section, we thus try the following finite-size scaling form in the critical region

$$\overline{Y_q(L,T)} = L^{-\tilde{\tau}(q)}\Phi[(T-T_c)L^{1/\nu}]. \tag{43}$$

For $T<T_c$, the convergence to finite values $\overline{Y_q(L=\infty,T)}$ in the $L\to\infty$ limit yields

$$\overline{Y_q(L=\infty,T)} = (T_c-T)^{\tilde{\beta}(q)} \text{ with } \tilde{\beta}(q)=\nu\tilde{\tau}(q). \tag{44}$$

This relation between the multifractal exponents $\tilde{\tau}(q)$ and the critical exponents $\tilde{\beta}(q)$ and ν is well known for the Anderson transitions (see the reviews [23,24]). Our results for $T<T_c$ are shown on Fig. 7 for (a) $q=2$ and (b) $q=3$ with the value $\nu=2$. This value is one of the two values $\nu\sim 2$ and $\nu\sim 4$

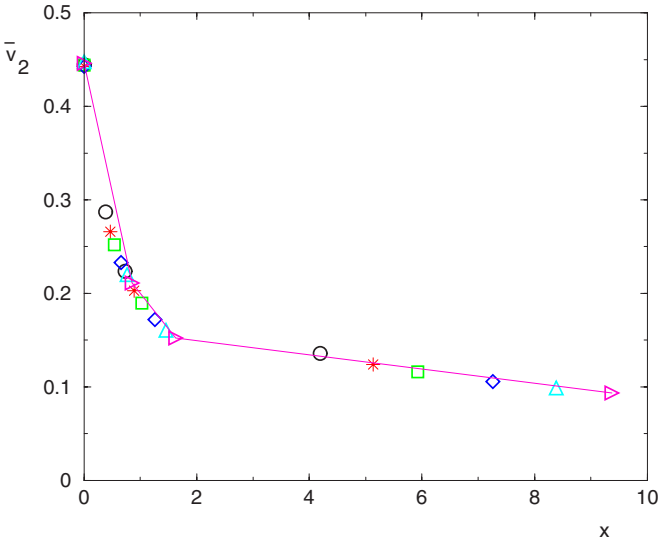

FIG. 8. (Color online) Finite-size scaling ($T>T_c$) of $\overline{v_2}=L^{\tilde{\gamma}(2)}\overline{Y_2}$ as a function of $x=(T-T_c)L^{1/\nu}$ with the value $\nu=2$ and for the sizes $L=12(\bigcirc)$, $18(*)$, $24(\square)$, $36(\diamond)$, $48(\triangle)$, and $60(\triangleright)$; see Eq. (43).

found previously in the literature for other observables [39,40,43].

For $T>T_c$, the results of the finite-size scaling form of Eq. (43) are shown on Fig. 8 for $q=2$ with the value $\nu=2$. Note that the matching between the finite-size scaling form of Eq. (43) and the asymptotic behavior in the delocalized phase [Eq. (13)] yields a diverging amplitude $A(T)$ in Eq. (13) for $q>1$

$$\overline{Y_q(L,T>T_c)} \sim \frac{A(T)}{L^{(3/2)(q-1)}} \tag{45}$$

with

$$A(T) \sim (T-T_c)^{-\nu(q-1)[3/2-\tilde{D}(q)]}.$$

Our data thus points towards a correlation length exponent $\nu\sim 2$ above and below T_c, i.e., toward a value very close to the general lower bound $\nu \geqslant 2/d=2$ of disordered systems [49].

VII. CONCLUSION

In this paper, we have found that the directed polymer in a random medium of dimension 1+3 exhibits multifractal properties at the critical localization-delocalization transition. We have numerically studied the statistics of the $Y_q(L)$ [see Eqs. (8) and (10)], which are the dynamical analogs of the inverse participation ratios of Anderson localization quantum models [23,24,26]. Our results are very close to the Evers-Mirlin scenario [21,26] for the Anderson transitions case. In particular, we have found that the generalized dimensions $D(q)$ and $\tilde{D}(q)$ for typical and disorder averaged values coincide for $q<q_c\sim 2$ but differ for $q>q_c$, and that the probability distributions of $y=Y_q(L)/Y_q^{\mathrm{typ}}(L)$ over the samples becomes scale invariant with a power-law tail $1/y^{1+x_q}$. We have also measured the corresponding typical singularity spectrum $f(\alpha)$, which starts at the value $\alpha_{\min}=D(+\infty)\sim 0.77$, and ends at $\alpha_{\max}=+\infty$. Off-critical results lead, through a finite size scaling analysis, to a value $\nu\sim 2$ for the correlation length exponent on both sides of the transition.

Finally, our numerical results, in particular the scale invariant shape of the histogram of $\ln Y_2(L)$ shown on Fig. 3(a), strongly support the equality $T_c=T_2(d=3)$ [see Eq. (5) and the corresponding discussion].

Since the directed polymer in a random medium can be mapped onto a growth model in the Kardar-Parisi-Zhang universality class [30], multifractality is also expected to show up at the critical point of these growth models. More generally, the present study confirms that it may be interesting to characterize the critical points of quenched disordered models by their multifractal properties.

ACKNOWLEDGMENT

We thank F. Iglói for drawing our attention to many relevant references.

[1] T. C. Halsey, M. H. Jensen, L. P. Kadanoff, I. Procaccia, and B. I. Shraiman, Phys. Rev. A **33**, 1141 (1986).
[2] G. Paladin and A. Vulpiani, Phys. Rep. **156**, 147 (1987).
[3] H. E. Stanley and P. Meakin, Nature (London) **335**, 405 (1988).
[4] *Fractals in Physics*, edited by A. Aharony and J. Feder, Essays in honour of B. B. Mandelbrot (North-Holland, Amsterdam, 1990).
[5] P. Meakin, *Fractals, Scaling and Growth Far From Equilibrium* (Cambridge University Press, Cambridge, UK, 1998).
[6] D. Harte, *Multifractals, Theory and Applications* (Chapman and Hall, New York, 2001).
[7] B. Duplantier, *Conformal Random Geometry*, Les Houches, Session LXXXIII, 2005, Mathematical Statistical Physics, edited by A. Bovier *et al.* (Elsevier, Amsterdam, 2006), p. 101.
[8] A. W. W. Ludwig, Nucl. Phys. B **330**, 639 (1990).
[9] J. L. Jacobsen and J. L. Cardy, Nucl. Phys. B **515**, 701 (1998).
[10] T. Olson and A. P. Young, Phys. Rev. B **60**, 3428 (1999).
[11] G. Palágyi, C. Chatelain, B. Berche, and F. Iglói, Eur. Phys. J. B **13**, 357 (2000).
[12] C. Chatelain and B. Berche, Nucl. Phys. B **572**, 626 (2000).
[13] N. Sourlas, Europhys. Lett. **3**, 1007 (1987).
[14] M. J. Thill and H. J. Hilhorst, J. Phys. I **6**, 67 (1996).
[15] G. Parisi and N. Sourlas, Phys. Rev. Lett. **89**, 257204 (2002).
[16] J. Kisker and A. P. Young, Phys. Rev. B **58**, 14397 (1998); F. Igloi, R. Juhasz, and H. Rieger, *ibid.* **61**, 11552 (2000).
[17] F. Wegner, Z. Phys. B **36**, 209 (1980).
[18] C. Castellani and L. Peliti, J. Phys. A **19**, L429 (1986).

[19] M. Schreiber and H. Grussbach, Phys. Rev. Lett. **67**, 607 (1991); H. Grussbach and M. Schreiber, Phys. Rev. B **51**, 663 (1995).
[20] T. Terao, Phys. Rev. B **56**, 975 (1997).
[21] A. Mildenberger, F. Evers, and A. D. Mirlin, Phys. Rev. B **66**, 033109 (2002).
[22] A. D. Mirlin, Y. V. Fyodorov, A. Mildenberger, and F. Evers, Phys. Rev. Lett. **97**, 046803 (2006).
[23] M. Janssen, Int. J. Mod. Phys. A **8**, 943 (1994); M. Janssen, Phys. Rep. **295**, 1 (1998).
[24] B. Huckestein, Rev. Mod. Phys. **67**, 357 (1995).
[25] C. C. Chamon, C. Mudry, and X.-G. Wen, Phys. Rev. Lett. **77**, 4194 (1996); H. E. Castillo, C. C. Chamon, E. Fradkin, P. M. Goldbart, and C. Mudry, Phys. Rev. B **56**, 10668 (1997); D. Carpentier and P. Le Doussal, Phys. Rev. E **63**, 026110 (2001).
[26] F. Evers and A. D. Mirlin, Phys. Rev. Lett. **84**, 3690 (2000); A. D. Mirlin and F. Evers, Phys. Rev. B **62**, 7920 (2000).
[27] W. Pook and M. Janssen, Z. Phys. B: Condens. Matter **82**, 295 (1991).
[28] B. Huckestein and L. Schweitzer, Phys. Rev. Lett. **72**, 713 (1994); B. Huckestein and R. Klesse, Phys. Rev. B **55**, R7303 (1997); T. Brandes, B. Huckestein, and L. Schweitzer, Ann. Phys. **5**, 633 (1996).
[29] F. Evers, A. Mildenberger, and A. D. Mirlin, Phys. Rev. B **64**, 241303 (2001).
[30] T. Halpin-Healy and Y.-C. Zhang, Phys. Rep. **254**, 215 (1995).
[31] S. Mukherji and S. M. Bhattacharjee, Phys. Rev. B **53**, R6002 (1996).
[32] B. Derrida and H. Spohn, J. Stat. Phys. **51**, 817 (1988).
[33] M. Mézard, J. Phys. (France) **51**, 1831 (1990).
[34] P. Carmona and Y. Hu, Probab. Theory Relat. Fields **124**, 431 (2002); P. Carmona and Y. Hu, e-print arXiv:math.PR/0601670.
[35] F. Comets, T. Shiga, and N. Yoshida, Bernoulli **9**, 705 (2003).
[36] V. Vargas, e-print arXiv:math.PR/0603233.
[37] J. Z. Imbrie and T. Spencer, J. Stat. Phys. **52**, 609 (1988).
[38] J. Cook and B. Derrida, J. Stat. Phys. **57**, 89 (1989).
[39] J. M. Kim, A. J. Bray, and M. A. Moore, Phys. Rev. A **44**, R4782 (1991).
[40] B. Derrida and O. Golinelli, Phys. Rev. A **41**, 4160 (1990).
[41] M. R. Evans and B. Derrida, J. Stat. Phys. **69**, 427 (1992).
[42] C. Monthus and T. Garel, Phys. Rev. E **74**, 011101 (2006).
[43] C. Monthus and T. Garel, Eur. Phys. J. B **53**, 39 (2006).
[44] B. Mandelbrot, Physica A **163**, 306 (1990); J. Stat. Phys. **110**, 739 (2003).
[45] A. B. Chhabra and K. R. Sreenivasan, Phys. Rev. A **43**, 1114 (1991).
[46] M. H. Jensen, G. Paladin, and A. Vulpiani, Phys. Rev. E **50**, 4352 (1994).
[47] T. C. Halsey, K. Honda, and B. Duplantier, J. Stat. Phys. **85**, 681 (1996); T. C. Halsey, B. Duplantier, and K. Honda, Phys. Rev. Lett. **78**, 1719 (1997).
[48] A. Chhabra and R. V. Jensen, Phys. Rev. Lett. **62**, 1327 (1989).
[49] J. T. Chayes, L. Chayes, D. S. Fisher, and T. Spencer, Phys. Rev. Lett. **57**, 2999 (1986).